Spatially-specific working memory activity in the human superior colliculus

Masih Rahmati,[1,2]

Kevin DeSimone,[1,2]

Clayton E. Curtis,[1,3]

Kartik K. Sreenivasan[2]

1. Department of Psychology, New York University, New York, NY 10003, USA

2. Division of Science and Mathematics, New York University Abu Dhabi, Abu Dhabi, UAE

3. Center for Neural Science, New York University, New York, NY 10003, USA

Corresponding Author: Kartik Sreenivasan, New York University Abu Dhabi, Computational Research Building (A2), Office 175, Abu Dhabi, UAE; kartik.sreenivasan@nyu.edu

Keywords: working memory, fMRI, modeling, human, retinotopy, saccades

ABSTRACT

Theoretically, working memory (WM) representations are encoded by population activity of neurons with distributed tuning across the stored feature. Here, we leverage computational neuroimaging approaches to map the topographic organization of human superior colliculus (SC) and model how population activity in SC encodes WM representations. We first modeled receptive field properties of voxels in SC, deriving a detailed topographic organization resembling the primate SC. Neural activity within human SC persisted throughout a retention interval of several types of modified memory-guided saccade tasks. Assuming an underlying neural architecture of the SC based on its retinotopic organization, we used an encoding model to show that the pattern of activity in human SC represents locations stored in WM. Our tasks and models allowed us to dissociate the locations of visual targets and the spatial metrics of memory-guided saccades from the spatial locations stored in WM, thus confirming that human SC represents true WM information. These data have several important implications. They add the SC to a growing number of cortical and subcortical brain areas that form distributed networks supporting WM functions. Moreover, they specify a clear neural mechanism by which topographically organized SC encodes WM representations.

NEW & NOTEWORTHY

Using computational neuroimaging approaches, we mapped the topographic organization of human superior colliculus (SC) and modeled how population activity in SC encodes working memory (WM) representations, rather than simpler visual or motor properties that have been traditionally associated with the laminar maps in the primate SC. Together, these data both position the human SC into a distributed network of brain areas supporting WM and elucidate the neural mechanisms by which the SC supports WM.

INTRODUCTION

We have known for decades that working memory (WM), a critical building block for higher cognition, relies on the persistent activity of neurons selective for the memoranda (Funahashi et al. 1989; Miller et al. 1996). More recent theoretical work suggests that WM features are encoded by the joint activity of large numbers of neurons with tunings that span the memorized feature space (Ma et al. 2014). Evidence from human studies using functional magnetic resonance imaging (fMRI), which allows for the simultaneous measurement of brain activity at scales that tile the space of neural population, supports the notion that macro-level distributed patterns of activity encode WM representations (Christophel et al. 2012; Ester et al. 2015; Sreenivasan et al. 2014). Computational model-based methods designed to identify these information-containing patterns demonstrate that WM representations are present in a surprising number of cortical brain regions (Sreenivasan and D'Esposito 2019). The success of these methods depend both on how encoding of the feature is distributed across a neural population (e.g., how visual space is distributed over V1) and how precisely aggregate voxel-wise measures of neural activity are feature-tuned (Brouwer and Heeger 2009; Naselaris et al. 2011; Sreenivasan and D'Esposito 2019). It follows that WM representations of visual space are robustly encoded in areas with systematic retinotopic organization, like early visual cortex (Rahmati et al. 2018; Sprague et al. 2014), and to lesser extents in areas with coarse topographic organization, like frontal and parietal cortex (Jerde et al. 2012; Mackey et al. 2017).

In this study, we focus on a subcortical structure, the human superior colliculus (SC), and test its potential role in spatial WM. We are motivated by the growing appreciation for the important role that subcortical regions play in cognition (Halassa and Kastner 2017), the well-established topography of the macaque SC (Cynader and Berman 1972; Goldberg and Wurtz 1972), and the above-mentioned recent developments in modeling fMRI measures of population activity. Traditionally, the SC mediates orienting behaviors (e.g., gaze shifts) by coordinating activity between two tightly registered eye-centered topographic maps: a map representing input from the visual system and a map representing motor output in the form of the angle and amplitude of saccades (Gandhi and Katnani 2011; Sparks 2002; Wurtz and Albano 1980). However, two recent lines of evidence argue against a strictly visuomotor-centric model of SC function. First, pharmacological inactivation of the macaque SC motor map induces a form of visual neglect akin to extinction, but does not cause anopsia (i.e., visual field defects) or paresis (i.e., deficits in voluntary oculomotion) (Lovejoy and Krauzlis 2010; McPeek and Keller 2004; Zénon and Krauzlis 2012). Second, neural activity in the cat and macaque SC motor map encodes the spatiotopic locations of a behavioral goal, rather than the specific metrics of the saccade to the goal (Bergeron et al. 2003; Freedman and Sparks 1997). Therefore, the functional role of the SC cannot be explained simply in terms of visual input or motor output. Instead, the SC may integrate signals computed throughout the brain into a common topographical organization, acting as a staging area for organizing flexible and goal-oriented behavior into a map of space that is weighted by bottom-up salience and top-down goal-relevance (Fecteau and Munoz 2006). Indeed, studies that use memory-guided saccade (MGS) tasks to dissociate visual and saccade related activity often observe delay period activity in macaque SC (Shen et al. 2011), consistent with the notion that the SC plays a role in spatial WM.

Here, we leverage computational neuroimaging approaches to 1) map the topographic organization of human SC, and 2) assuming an underlying neural architecture based on this topography, model how population activity in SC encodes WM representations disentangled from simple visual or motor components.

MATERIALS AND METHODS

A detailed description of the experimental methods, supplemental results and figures, and experimental data are available at https://osf.io/mkgd2/.

Subjects

Six subjects (ages 27-49; 5 male) participated in the study approved by the New York University Committee on Activities Involving Human Subjects and the New York University Abu Dhabi Institutional Review Board.

Procedures

MRI data was acquired in the Center for Brain Imaging at New York University with a 3-Tesla Siemens Prisma MRI scanner scanner using a 32-channel head coil. Twenty functional series of 120 volumes were collected for the retinotopic mapping task and twenty functional runs (except for one subject from whom we collected ten runs) of 232 volumes were collected for the WM task. Stimuli viewed stimuli projected onto a screen located at the end of the scanner bore. We measured eye gaze constantly throughout the experiment to quantify performance of visual and memory guided saccades.

Population receptive field (pRF) experiment: The pRF model provides a description of each voxel's BOLD response in terms of a retinotopic location and extent. Subjects viewed contrast reversing checkerboard-patterned bars that swept across the visual field. We modeled each SC voxel in terms of a Gaussian pRF (Fig. 1A) using methods (Dumoulin and Wandell 2008) and tools previously described (DeSimone et al. 2015).

Model-based spatial WM experiment: In order to measure spatial WM representations in the SC, we imaged the brain while subjects maintained a location in WM during a memory retention interval and made saccades to indicate their recollection (Fig. 2A). Two task manipulations were designed to help us understand the nature of the information maintained in the SC during the memory delay. First, after each delay subjects made an intermediate VGS which was designed to prevent a simple maintenance of saccade metrics required to reach the memorized target (Fig. 2A/B). Second, the color of the visual cue indicated what type of geometric transformation was required to remap its location to the goal of a later MGS (Fig. 2A). The various transformations moved the task-relevant location — the goal of the MGS — to a position in visual space that was independent of the retinal position of the visual stimulus and thus prevented a simple storage of the location of the visual target. Together, we aimed to eliminate simply visual and/or motor components while honing in on WM representations of visual space.

To reconstruct a representation of spatial WM from the pattern of SC activity during the memory delay, we used a spatial inverted encoding model (IEM; Fig. 3A) (Brouwer and Heeger 2009). Briefly, we trained the model based on the delay period patterns of SC activity during the MGS

condition that required no target transformation and cross-validated the model using only data from the delay periods of trials that required target transformations. This further ensured that simple visual and motor representations could not drive our results. To quantify the goodness of our reconstructions, we used a modified version of the representational fidelity metric (Sprague et al. 2016) and computed significance using shuffled data and bootstrapping procedures.

RESULTS

Retinotopic mapping

Following our pRF mapping procedures (Fig. 1A), we overlaid the modeled receptive field properties of voxels in the SC of a representative subject in Figure 1B (individual subjects in *Supplementary Fig. 1*). We found orthogonal polar angle and eccentricity representations of the visual field along the SC. The topography revealed a graded upper-to-lower visual field representation along the medial-to-lateral axis of the SC, and a graded foveal-to-peripheral visual field representation along the anterior-to-posterior axis. The SC pRFs largely tiled the contralateral visual field (Fig. 1C). Moreover, like in the macaque (Marino et al. 2008), we found a positive correlation between the size and eccentricity of pRF parameters in the SC (Pearson's r=0.52, p<0.0001; Fig. 1D). Overall, our model of the topographic structure of the human SC closely resembles that of the macaque (Cynader and Berman 1972; Goldberg and Wurtz 1972) and a previous report in humans (DeSimone et al. 2015).

Spatial working memory

The latency and precision of both visual and memory-guided saccades were similar to previous studies that used delayed saccade or antisaccade tasks (Curtis and Connolly 2008; Saber et al. 2015), despite the transformations and double saccades (Fig. 2C/D). The average BOLD signal in the retinotopically defined human SC persisted above pre-trial baseline during the memory period suggesting it may play an important role in WM (percent signal change; mean=0.04, 95% CI=[0.009 0.08], p<0.01; Fig. 2E). However, it was not lateralized with respect to the MGS target - a pattern incongruous with the clear lateralization of the SC RFs (Fig. 1C). This may be due to the intervening VGS target and complex transformations required by the task. Alternatively, averaging over many voxels may result in a measure that is too coarse to capture the population dynamics by which the SC encodes WM.

Motivated by our pRF findings, we used a multivoxel model of visual space (Fig. 3A) to test whether topographic patterns of activity in human SC encode WM locations. We assumed an underlying neural architecture based on the retinotopic organization of the voxels within SC, and modeled each voxel's response with a set of basis functions that tiled polar angular space. Our model of SC activity could accurately reconstruct the transformed location of the MGS, but not the locations of the visual target or the VGS location (Fig. 3B); SC population activity during the delay was spatially tuned only for the location of the MGS target (mean fidelity=0.0013, 95% CI=[0.0010 .0023] p<0.001; Fig. 3C). We found these effects at the individual level in five of six subjects (*Supplementary Fig. 2*), providing robust evidence for spatial WM encoding in human SC.

DISCUSSION

With fMRI, we show that the human SC has a similar topographic organization as the macaque SC, and during memory retention intervals its activity both persists and encodes spatial WM representations. Critically, the patterns of delay period activity we modeled did not encode retinal positions of past visual stimuli or planned saccades. The locations held in WM were abstract transformations of visually stimulated locations, and the visually-guided saccades negated strategies involving the maintenance of saccade metrics. Therefore, top-down signals targeting SC neurons with receptive fields matching the transformed locations may be the source of the population encoded responses we observed. Likely sources of these top-down influences include brain areas with direct connections to the SC, namely, prefrontal cortex, frontal eye field, and V1, each of which are known to support spatial WM functions (Armstrong et al. 2009; Everling and Johnston 2013; van Kerkoerle et al. 2017; Koval et al. 2011; Sommer and Wurtz 2001). However, it is unlikely that SC simply integrates cortical commands and relays them to brainstem oculomotor plants. Indeed, in the macaque, representations of visual priority emerge more rapidly in SC than in V1, indicating that feedback signals from SC may sculpt the gain of responses in cortex (White et al. 2017).

Our success depended on a model of well-defined spatial tuning of SC, where space is systematically distributed over hundreds of voxels, and an assumption that WM was encoded in the SC population response. Indeed, we have long appreciated that the population of SC neurons collectively codes for visual and motor behavior (Lee et al. 1988; McIlwain 1991), but the actual mechanism by which the population activity is combined remains unknown. As suggested by computational models of perception that posit neural populations encode a probability distribution over sensory features (Ma et al. 2006), the population response in SC may encode the probability of a prioritized, including a remembered, location (Fecteau and Munoz 2006; Kim and Basso 2010). Bayesian decoding models of fMRI population responses (van Bergen et al. 2015) may be able to test this hypothesis in the human SC.

Finally, topographic organization provides computational efficiency (Kaas 1997) and the tight registration between superficial visual and deeper motor layers of SC makes the transformations between vision and action efficient (Sparks 1999). If we extend this idea to the large network of retinotopically organized brain areas that have been associated with spatial WM (Christophel et al. 2017), then retinotopy enables an efficient interface among these brain areas, including the SC. Future research should address how these cortical and subcortical brain areas differ in their support of WM. Perhaps, they utilize similar mechanisms, but differences may emerge due to their areal input-output connections, parameters that govern local circuit-level dynamics, or more broadly factors related to behavioral goals and task contexts (Sreenivasan and D'Esposito 2019).

ACKNOWLEDGEMENTS

We thank Jeffrey Kravitz for processing and analyzing the eye tracking data. We thank New York University's Center for Brain Imaging for technical support.

GRANTS

This research was supported by the National Eye Institute (R01 EY-016407 to C.E. Curtis) and by an NYU Global Seed Grants for Collaborative Research (K.K. Sreenivasan and C.E. Curtis).

DISCLOSURES

No conflicts of interest, financial or otherwise, are declared by the authors.

AUTHOR CONTRIBUTIONS

K.D., C.E.C., and K.K.S. conceived and designed research; K.D. performed experiments; M.R. and K.D. analyzed data; M.R., K.D., C.E.C., and K.K.S. interpreted the results of experiments, prepared figures, drafted the manuscript, and approved the final version of the manuscript.

REFERENCES

Armstrong KM, **Chang MH**, **Moore T**. Selection and maintenance of spatial information by frontal eye field neurons. *J Neurosci* 29: 15621–15629, 2009.

van Bergen RS, **Ma WJ**, **Pratte MS**, **Jehee JFM**. Sensory uncertainty decoded from visual cortex predicts behavior. *Nat Neurosci* 18: 1728–1730, 2015.

Bergeron A, **Matsuo S**, **Guitton D**. Superior colliculus encodes distance to target, not saccade amplitude, in multi-step gaze shifts. *Nat Neurosci* 6: 404–413, 2003.

Brouwer GJ, **Heeger DJ**. Decoding and reconstructing color from responses in human visual cortex. *J Neurosci* 29: 13992–14003, 2009.

Christophel TB, **Hebart MN**, **Haynes J-D**. Decoding the contents of visual short-term memory from human visual and parietal cortex. *J Neurosci* 32: 12983–12989, 2012.

Christophel TB, **Klink PC**, **Spitzer B**, **Roelfsema PR**, **Haynes J-D**. The Distributed Nature of Working Memory. *Trends Cogn Sci* 21: 111–124, 2017.

Curtis CE, **Connolly JD**. Saccade Preparation Signals in the Human Frontal and Parietal Cortices. *Journal of Neurophysiology* 99: 133–145, 2008.

Cynader M, **Berman N**. Receptive-field organization of monkey superior colliculus. *J Neurophysiol* 35: 187–201, 1972.

DeSimone K, **Viviano JD**, **Schneider KA**. Population Receptive Field Estimation Reveals New Retinotopic Maps in Human Subcortex. *J Neurosci* 35: 9836–9847, 2015.

Dumoulin SO, **Wandell BA**. Population receptive field estimates in human visual cortex. *Neuroimage* 39: 647–660, 2008.

Ester EF, **Sprague TC**, **Serences JT**. Parietal and Frontal Cortex Encode Stimulus-Specific Mnemonic Representations during Visual Working Memory. *Neuron* 87: 893–905, 2015.

Everling S, **Johnston K**. Control of the superior colliculus by the lateral prefrontal cortex. *Philos Trans R Soc Lond B Biol Sci* 368: 20130068, 2013.

Fecteau JH, **Munoz DP**. Salience, relevance, and firing: a priority map for target selection. *Trends Cogn Sci* 10: 382–390, 2006.

Freedman EG, **Sparks DL**. Eye-head coordination during head-unrestrained gaze shifts in rhesus monkeys. *J Neurophysiol* 77: 2328–2348, 1997.

Funahashi S, **Bruce CJ**, **Goldman-Rakic PS**. Mnemonic coding of visual space in the monkey's dorsolateral prefrontal cortex. *J Neurophysiol* 61: 331–349, 1989.

Gandhi NJ, **Katnani HA**. Motor functions of the superior colliculus. *Annu Rev Neurosci* 34: 205–231, 2011.

Goldberg ME, **Wurtz RH**. Activity of superior colliculus in behaving monkey. I. Visual receptive fields of single neurons. *J Neurophysiol* 35: 542–559, 1972.

Halassa MM, **Kastner S**. Thalamic functions in distributed cognitive control. *Nat Neurosci* 20: 1669–1679, 2017.

Jerde TA, **Merriam EP**, **Riggall AC**, **Hedges JH**, **Curtis CE**. Prioritized maps of space in human frontoparietal cortex. *J Neurosci* 32: 17382–17390, 2012.

Kaas JH. Topographic maps are fundamental to sensory processing. *Brain Res Bull* 44: 107–112, 1997.

van Kerkoerle T, **Self MW**, **Roelfsema PR**. Layer-specificity in the effects of attention and working memory on activity in primary visual cortex. *Nat Commun* 8: 13804, 2017.

Kim B, **Basso MA**. A probabilistic strategy for understanding action selection. *J Neurosci* 30: 2340–2355, 2010.

Koval MJ, **Lomber SG**, **Everling S**. Prefrontal cortex deactivation in macaques alters activity in the superior colliculus and impairs voluntary control of saccades. *J Neurosci* 31: 8659–8668, 2011.

Lee C, **Rohrer WH**, **Sparks DL**. Population coding of saccadic eye movements by neurons in the superior colliculus. *Nature* 332: 357–360, 1988.

Lovejoy LP, **Krauzlis RJ**. Inactivation of primate superior colliculus impairs covert selection of signals for perceptual judgments. *Nat Neurosci* 13: 261–266, 2010.

Mackey WE, **Winawer J**, **Curtis CE**. Visual field map clusters in human frontoparietal cortex. *Elife* 6, 2017.

Marino RA, **Rodgers CK**, **Levy R**, **Munoz DP**. Spatial relationships of visuomotor transformations in the superior colliculus map. *J Neurophysiol* 100: 2564–2576, 2008.

Ma WJ, **Beck JM**, **Latham PE**, **Pouget A**. Bayesian inference with probabilistic population codes. *Nat Neurosci* 9: 1432–1438, 2006.

Ma WJ, **Husain M**, **Bays PM**. Changing concepts of working memory. *Nature Neuroscience* 17: 347–356, 2014.

McIlwain JT. Distributed spatial coding in the superior colliculus: a review. *Vis Neurosci* 6: 3–13, 1991.

McPeek RM, **Keller EL**. Deficits in saccade target selection after inactivation of superior colliculus. *Nat Neurosci* 7: 757–763, 2004.

Miller EK, **Erickson CA**, **Desimone R**. Neural mechanisms of visual working memory in prefrontal cortex of the macaque. *J Neurosci* 16: 5154–5167, 1996.

Naselaris T, **Kay KN**, **Nishimoto S**, **Gallant JL**. Encoding and decoding in fMRI. *Neuroimage* 56: 400–410, 2011.

Rahmati M, **Saber GT**, **Curtis CE**. Population Dynamics of Early Visual Cortex during Working Memory. *J Cogn Neurosci* 30: 219–233, 2018.

Saber GT, **Pestilli F**, **Curtis CE**. Saccade planning evokes topographically specific activity in the dorsal and ventral streams. *J Neurosci* 35: 245–252, 2015.

Shen K, **Valero J**, **Day GS**, **Paré M**. Investigating the role of the superior colliculus in active vision with the visual search paradigm. *Eur J Neurosci* 33: 2003–2016, 2011.

Sommer MA, **Wurtz RH**. Frontal eye field sends delay activity related to movement, memory, and vision to the superior colliculus. *J Neurophysiol* 85: 1673–1685, 2001.

Sparks DL. Conceptual issues related to the role of the superior colliculus in the control of gaze. *Curr Opin Neurobiol* 9: 698–707, 1999.

Sparks DL. The brainstem control of saccadic eye movements. *Nat Rev Neurosci* 3: 952–964, 2002.

Sprague TC, **Ester EF**, **Serences JT**. Reconstructions of information in visual spatial working memory degrade with memory load. *Curr Biol* 24: 2174–2180, 2014.

Sprague TC, **Ester EF**, **Serences JT**. Restoring Latent Visual Working Memory Representations in Human Cortex. *Neuron* 91: 694–707, 2016.

Sreenivasan KK, **D'Esposito M**. The what, where and how of delay activity. *Nat Rev Neurosci* 20: 466–481, 2019.

Sreenivasan KK, **Vytlacil J**, **D'Esposito M**. Distributed and dynamic storage of working memory stimulus information in extrastriate cortex. *J Cogn Neurosci* 26: 1141–1153, 2014.

White BJ, **Kan JY**, **Levy R**, **Itti L**, **Munoz DP**. Superior colliculus encodes visual saliency before the primary visual cortex. *Proc Natl Acad Sci U S A* 114: 9451–9456, 2017.

Wurtz RH, **Albano JE**. Visual-motor function of the primate superior colliculus. *Annu Rev Neurosci* 3: 189–226, 1980.

Zénon A, **Krauzlis RJ**. Attention deficits without cortical neuronal deficits. *Nature* 489: 434–437, 2012.

FIGURES AND CAPTIONS

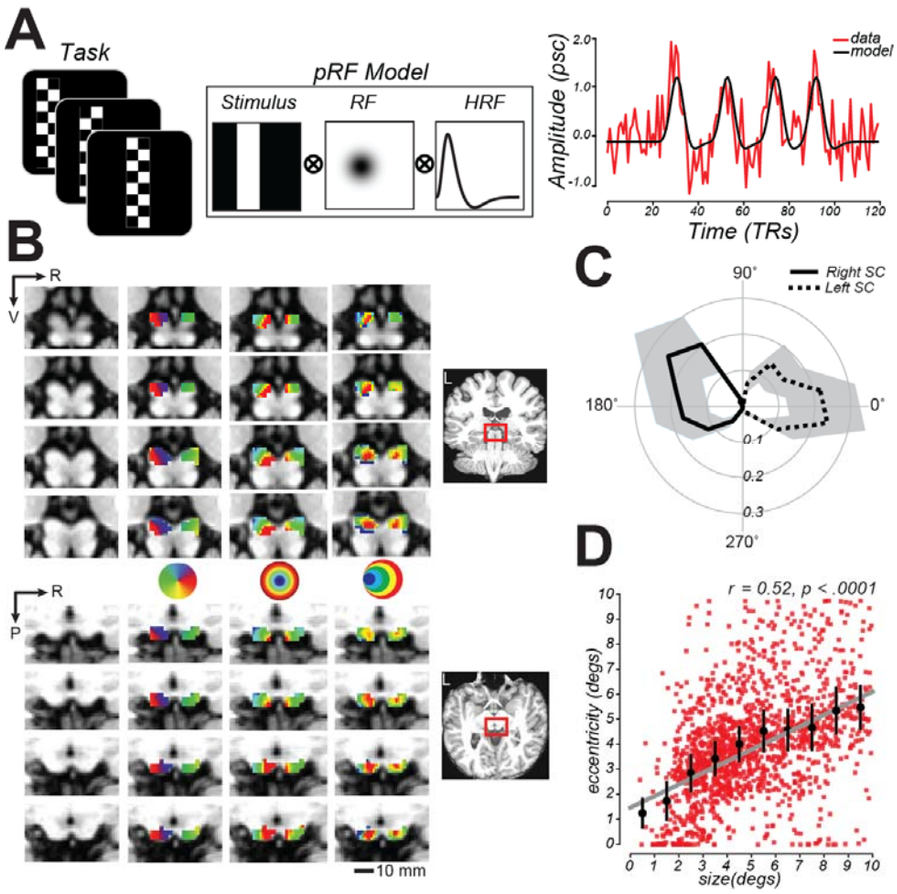

Fig. 1. Topographic mapping of human superior colliculus (SC). ***A.*** To model voxel population receptive fields (pRF), subjects viewed bars of contrast reversing checkerboards that swept across the visual field. Bar positions over time converted into binary apertures were projected onto 2D Gaussian model of a receptive field (RF) and convolved with a hemodynamic response function (HRF). To the right, a single sample voxel in SC is plotted for one run. ***B.*** Coronal (top) and axial (bottom) slices through the human SC (red box inset). R=right; P=posterior; V=ventral. From left-to-right, the columns depict the T1 anatomy, polar angle, eccentricity, and size parameter maps of an example subject (S5; thresholded at $r^2 \geq 0.1$). The colored circles are visual field keys. ***C.*** Radial histograms of pRF polar angle in SC demonstrate strong contralateral coverage of the visual field. ***D.*** pRF size in the SC increased linearly with eccentricity. Red squares = SC voxels from all subjects; Black dots = binned means (± SEM); Gray line = linear fit.

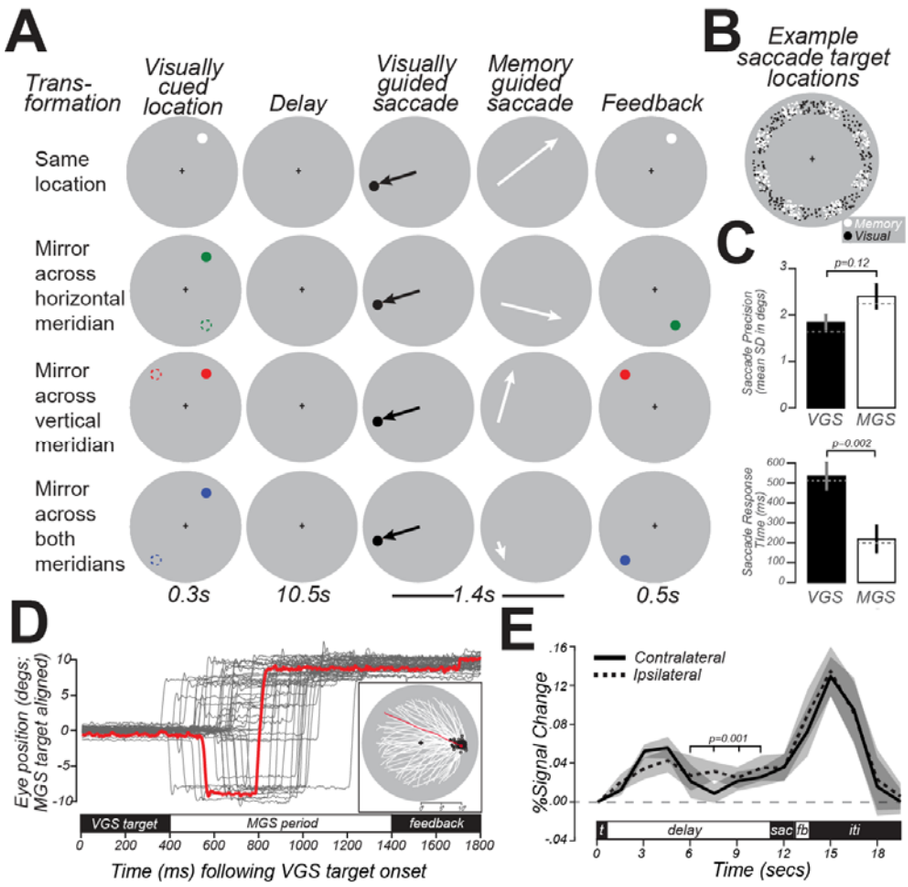

Fig. 2. Task schematic, behavioral data, and delay-period activity in human SC. ***A.*** Schematic of four types of MGS trials. In each condition, trials began with a brief visual target located in the periphery (colored dots; left column). Following a delay, subjects made a VGS to a target whose location was unpredictable. Then, subjects immediately made a MGS to a location based on the initial visual target. In one condition, the MGS was to the visual target. In the other conditions, the MGS was made to simple geometric transformations of the visual target (dashed circles, left column; for reference here but not displayed). These included mirror transformations across each meridian and both meridians. The color of the visually-cued target indicated the type of transformation. Feedback was provided after the MGS with a visual stimulus at the correct location. Because of the VGS, the metrics of the MGS could not be predicted. The transformations dissociated the goal of the MGS from the visually-stimulated retinal position. ***B.*** Locations of VGS and MGS targets were distributed 9-11˚ in the periphery. ***C.*** VGS were slightly more accurate and significantly slower than MGS. Bars=mean (±SEM); Gray dashed line=median. ***D.*** Example eye-tracking traces (gray lines) from a subject during one scanner session. All trials are rotated such that despite the various transformations of the visual target location, all MGS targets are rotated to a location 10˚ to the right. The red trace highlights an example trial. In the inset, we re-plot only the MGS trajectories (white lines), which start from a wide variety of peripheral locations following the VGS but converge and end (black circles) near the aligned MGS target location. The red trace highlights an example trial. ***E.*** Group-averaged (±SEM) BOLD signal in SC voxels persisted significantly above pre-trial baseline (gray dashed line) during the delay period for trials when the MGS target was in the contralateral and ipsilateral hemifield. The delay was defined as the average of the last four TRs in the delay period, identified by the bracket above the time courses.

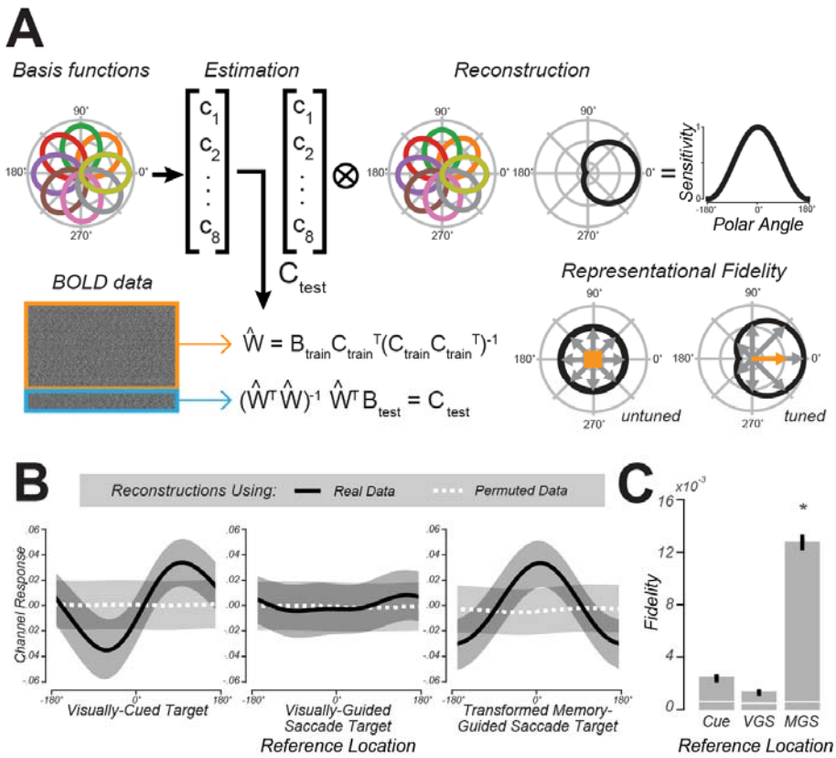

Fig. 3. Inverted encoding model (IEM) and results. **A.** Using a standard IEM, we calculated regression weights (W) from a training set of BOLD data (B_{train}; orange box) and corresponding hypothetical channel coefficients (C_{train}) represented by eight evenly spaced radial basis functions, each tuned to a specific angle. We calculated the contribution of each basis function in the final reconstruction (C_{test}) by linearly combining a new set of BOLD data (B_{test}; blue box) and the inverse of the regression weights. To reconstruct a representation of visual space, we used a linear combination of all basis functions, each weighted by its corresponding contribution in C_{test}. To the right, we unwrap the curve to show a sample sensitivity profile across angles in visual space. We calculated representational fidelity — a metric for the goodness of reconstructions — as the vector mean of a set of unit vectors around different angles, each weighted by the reconstructed sensitivity at that position. Displayed are examples of poor/untuned, and good/tuned representations. **B.** We used delay period activity in human SC to reconstruct visual space. From left to right: the average reconstructed sensitivity (±SEM) in visual space aligned to the visually-cued target, VGS target, and MGS target locations, respectively. In each panel, all trials are aligned to the corresponding reference location centered at 0˚. The dashed white lines depict reconstructions from BOLD data with the trial labels permuted. **C.** Representational fidelity (±SEM) corresponding to three reference locations, compared to shuffled data (white lines). Note that the SC population activity during the delay is largely tuned for the visual-spatial location of the MGS ($p<10^{-18}$), not the visual target or VGS.